The American Journal of Pathology, Vol. 187, No. 1, January 2017

The American Journal of
PATHOLOGY
ajp.amjpathol.org

TUMORIGENESIS AND NEOPLASTIC PROGRESSION

Argininosuccinate Synthetase 1 Loss in Invasive Bladder Cancer Regulates Survival through General Control Nonderepressible 2 Kinase—Mediated Eukaryotic Initiation Factor 2α Activity and Is Targetable by Pegylated Arginine Deiminase

Divya Sahu,* Sounak Gupta,* Andrew M. Hau,* Kazufumi Nakashima,* Mariah Z. Leivo,* Stephen C. Searles,* Paul Elson,† John S. Bomalaski,‡ Darren E. Casteel,§ Gerry R. Boss,§ and Donna E. Hansel*

From the Departments of Pathology and Medicine,§ University of California at San Diego, La Jolla, California; the Lerner Research Institute,† Cleveland Clinic, Cleveland, Ohio; and Polaris Pharmaceuticals,‡ San Diego, California*

Accepted for publication September 1, 2016.

Address correspondence to Donna E. Hansel, M.D., Ph.D., Department of Pathology, University of California at San Diego, 9500 Gilman Dr., MC 0612, La Jolla, CA 92093. E-mail: dhansel@ucsd.edu.

Loss of argininosuccinate synthetase 1 (ASS1), a key enzyme for arginine synthesis, occurs in many cancers, making cells dependent on extracellular arginine and targetable by the arginine-degrading enzyme pegylated arginine deiminase (ADI-PEG 20). We evaluated ASS1 expression and effects of ASS1 loss in bladder cancer which, despite affecting >70,000 people in the United States annually, has limited therapies. ASS1 loss was identified in conventional and micropapillary urothelial carcinoma, small cell, and squamous cell carcinoma subtypes of invasive bladder cancer, as well as in T24, J82, and UM-UC-3 but not in 5637, RT112, and RT4 cell lines. ASS1-deficient cells showed preferential sensitivity to ADI-PEG 20, evidenced by decreased colony formation, reduced cell viability, and increased sub-G1 fractions. ADI-PEG 20 induced general control nonderepressible 2—dependent eukaryotic initiation factor 2α phosphorylation and activating transcription factor 4 and C/EBP homologous protein up-regulation, associated with caspase-independent apoptosis and autophagy. These effects were ablated with selective siRNA silencing of these proteins. ASS1 overexpression in UM-UC-3 or ASS1 silencing in RT112 cells reversed these effects. ADI-PEG 20 treatment of mice bearing contralateral flank UM-UC-3 and RT112 xenografts selectively arrested tumor growth in UM-UC-3 xenografts, which had reduced tumor size, reduced Ki-67, and increased terminal deoxynucleotidyl transferase-mediated dUTP nick-end labeling staining. This suggests that ASS1 loss occurs in invasive bladder cancer and is targetable by ADI-PEG 20. *(Am J Pathol 2017, 187: 200—213; http://dx.doi.org/10.1016/j.ajpath.2016.09.004)*

Identification of metabolic pathways that confer growth or survival advantages during cancer progression has emerged as a unique approach to determine potential novel therapeutic targets.[1] Arginine synthesis and utilization represents a unique metabolic target in cancer. In humans, arginine is a semiessential amino acid that is synthesized from citrulline in two steps of the urea cycle: citrulline and aspartate are converted to argininosuccinate via argininosuccinate

Supported by Case Western Reserve University/Cleveland Clinic CTSA grant UL1 RR024989 from the National Center for Research Resources, a KL2 career development award RR024990, and University of California at San Diego start-up funding (D.E.H.); Prevent Cancer Foundation Fellowship (D.S.); and AUA Urology Care Foundation Research Scholar Award (A.M.H.).

Disclosures: J.S.B. is an employee of Polaris Pharmaceuticals with stock options. Polaris Pharmaceuticals supplied the drug ADI-PEG 20.

http://dx.doi.org/10.1016/j.ajpath.2016.09.004

synthetase (ASS1), followed thereafter by conversion of argininosuccinate to arginine and fumarate via argininosuccinate lyase; the ASS1-catalyzed reaction is the rate-limiting step in this process.[2] Arginine is essential for production of proteins, polyamines, nitric oxide, urea, creatinine, proline, glutamate, and agmantine; hence, it plays a key role in tumor biology.[3] Loss of ASS1 occurs in some cancers such as hepatocellular carcinoma, melanoma, myxofibrosarcoma, mesothelioma, prostate cancer, and renal cancer, rendering the cancer cells dependent on extracellular arginine (arginine auxotrophs).[4] Despite its critical role in cell growth and function, ASS1 has been proposed to also function as a tumor-suppressor gene, thus explaining its paradoxical loss in cancer cells.[4]

Arginine-degrading enzymes, such as arginase and arginine deiminase (ADI), show promise as a novel therapy for cancers lacking ASS1.[5] ADI is derived from a mycobacterium and shows high affinity for arginine, thus effectively catabolizing arginine in the extracellular milieu. Pegylation of ADI (ADI-PEG 20; Polaris Pharmaceuticals, San Diego, CA) renders the enzyme less immunogenic, thereby increasing its pharmacokinetic half-life.[6] ADI-PEG 20 is currently being evaluated in a phase 3 trial for hepatocellular carcinoma and is under investigation for use in melanoma[7–9] and mesothelioma.[10] A number of other cancer types may also show response to ADI-PEG 20–directed therapy, including pancreatic cancer,[11] prostate cancer,[12] small cell lung cancer,[13] lymphoma,[4] and glioblastoma.[14]

We examined arginine metabolism in bladder cancer, a disease that affects >180,000 new patients worldwide each year, including >70,000 patients in the United States.[15,16] We assessed ASS1 loss in human bladder cancers and tested functional effects of arginine deprivation and ADI-PEG 20 *in vitro* and *in vivo*. Our results suggest that arginine deprivation may be a useful strategy for treating bladder cancer and show that ADI-PEG 20 functions through a novel signaling mechanism that includes the nutrient-sensing general control nonderepressible 2 (GCN2) kinase pathway that controls autophagy and apoptosis.

Materials and Methods

Patient Specimens and Tissue Microarray Construction

The study was approved by The Cleveland Clinic and the University of California, San Diego institutional review boards. Specimens included archived paraffin blocks from patients who underwent radical cystectomy or cystoprostatectomy for muscle-invasive bladder cancer (pathologic stage pT2 or greater) between November 1988 and May 2008. All specimens were re-reviewed by one of the authors (D.E.H.) for diagnostic accuracy. Whole sections were used to evaluate normal urothelium, and cancers were analyzed using tissue microarray that included four separate regions per specimen. Nineteen specimens were from patients who underwent radical cystectomy for non-neoplastic processes. Bladder cancers assessed for ASS1 expression included 148 invasive high-grade urothelial carcinomas, 27 micropapillary urothelial carcinomas, 39 pure squamous cell carcinomas, 19 pure adenocarcinomas, and 19 pure small cell carcinomas (SCCs).

IHC

Immunohistochemistry (IHC) was performed on 4-μm sections of formalin-fixed paraffin-embedded tissue using a Discovery XT automated stainer (Ventana Medical Systems, Tucson, AZ). Antigen retrieval consisted of incubation in CC1 buffer (Tris/borate/EDTA buffer, pH 8.0–8.5; Ventana Medical Systems) for 8 minutes at 95°C, 28 minutes at 100°C, and then an 8-minute cool down to room temperature. The slides were then incubated with an anti-ASS1 mouse monoclonal antibody (dilution 1:20; gift from Polaris Pharmaceuticals) for 60 minutes at room temperature, followed by three rinses in phosphate-buffered saline and application of secondary antibody (Ventana OmniMap anti-Mouse HRP) for 20 minutes at 37°C. Chromogenic development was performed using ChromoMap DAB (Ventana Medical Systems) for 5 minutes at room temperature. Slides were counterstained with Hematoxylin II and Bluing Reagent (Ventana Medical Systems) and visualized by light microscopy. The optimal antibody concentration was determined by testing different concentrations on control tissues on an automated stainer and chosen based on strong signal with minimum background. Semiquantitative analysis of IHC intensity was performed using a range of 0 (absent staining), 1+ (weak staining), 2+ (moderate staining), and 3+ (intense staining). Immunostaining in at least 10% of the cells was considered positive. Normal urothelium showed 2+ to 3+ staining and was used as an internal control when present; renal proximal tubules showed 3+ staining intensity and were used as an internal slide control in tissue microarray studies. Comparison of immunolabeling between populations was performed using the Fisher exact test.

Cell Lines, Arginine Deprivation, and ADI-PEG 20, 5-Aza Administration

RT4, SCaBER, UM-UC-3, T24, J82, and Jurkat cell lines were purchased from ATCC (Manassas, VA). RT112 and 5637 cells were a kind gift from Dr. P. Szlosarek (Queen Mary University of London, London, England) and immortalized normal urothelial UROtsa cells were obtained from Deutsche Sammlung fur Mikroorganismen und Zellkultur (Braunschweig, Germany). Cells were grown in RPMI-1640 (Gibco, Life Technologies, Grand Island, NY) supplemented with 10% fetal bovine serum (Gibco). For arginine deprivation, we used arginine-free RPMI-1640 (Sigma-Aldrich Corp., St. Louis, MO) supplemented with dialyzed fetal bovine serum (Life Technologies, Carlsbad, CA). All cell lines were maintained at 37°C in 5% CO_2.

ADI-PEG 20 was diluted in serum-free media and applied to cells as described below. For demethylation assays, J82 cells were treated with 0.3 μmol/L 5-azacytidine (5-Aza) (Sigma-Aldrich Corp.) for 10 days, with the drug replenished every 3 days. For citrulline (Sigma-Aldrich Corp.) rescue experiments, cells were treated with indicated concentrations for 48 hours before analysis.

Immunoblot Analysis, Plasmids, and siRNA

Whole-cell lysates were extracted with RIPA buffer containing protease and phosphatase inhibitor cocktails (Roche, Basel, Switzerland) and were subjected to Western blot analysis as previously described.[17] Proteins were separated on 4% to 15% gradient polyacrylamide–sodium dodecyl sulfate gels (Bio-Rad Laboratories, Inc., Hercules, CA), transferred to Supported Nitrocellulose membranes (Bio-Rad, Inc.) using a Bio-Rad Mini-PROTEAN Tetracell system, followed by incubation for 1 hour in a bovine serum albumin/Tween-20–based blocking solution. Primary antibodies included ASS1 (dilution 1:200) from Polaris Pharmaceuticals; and phosphorylated eukaryotic initiation factor 2 α (p-eIF2α; Ser51; dilution 1:1000), eIF2α (dilution 1:1000), GCN2 (dilution 1:1000), activating transcription factor 4 (ATF4; dilution 1:1000), C/EBP homologous protein (CHOP; dilution 1:1000), LC3A/B (dilution 1:1000), actin (dilution 1:1000), poly (ADP-ribose) polymerase (PARP), and pro- and cleaved-caspase 3, 7, and 9 (all dilutions 1:1000) from Cell Signaling Technology (Danvers, MA). Control lysates for PARP and caspase cleavage were from Cell Signaling Technology. Blots were incubated with primary antibody overnight and then were incubated for 1 hour with horseradish phosphatase–conjugated anti-rabbit or anti-mouse secondary antibodies (dilution 1:10,000; Jackson ImmunoResearch Laboratories, Inc., West Grove, PA). Blots were developed using the Enhanced Chemiluminescence Kit (Pierce, Thermo Fisher Scientific, Waltham, MA) followed by autoradiography. For ASS1 overexpression, Lipofectamine 3000 Reagent (Invitrogen, Life Technologies) was used to transfect an overexpression vector plasmid with cytomegalovirus promoter (ASS1/pCMV) (Origene, Rockville, MD) or empty vector plasmid after which a stable population was generated by selection with geneticin (Gibco). For ASS1, GCN2, ATF4, and CHOP siRNA and control transfection, the Lipofectamine RNAiMAX Reagent (Invitrogen, Life Technologies) was used to transfect either siGENOME pooled nontargeting control (NTC) siRNA or siGENOME SMARTpool gene-specific siRNA (all from GE Dharmacon, Lafayette, CO).

Colony Formation Assay

Cells were plated, allowed to attach overnight at 37°C, and then treated with either arginine-free medium or indicated concentrations of ADI-PEG 20 in complete medium. All media were replenished twice weekly. Colonies formed in 6 days for J82 cells, 10 days for UM-UC-3 and RT112 cells, and 11 days for 5637 cells. The colonies were fixed with 100% methanol at 4°C for 5 minutes, stained with 0.5% crystal violet for 30 minutes at room temperature, and washed twice in phosphate-buffered saline; they were then photographed and counted.

Cell Viability Assay

Cell viability was assessed using the Vybrant MTT Cell Proliferation Assay Kit (Molecular Probes, Life Technologies). Cells were plated onto 96-well plates and treated with indicated concentrations of ADI-PEG 20 for 48 hours before analysis. Results for test samples were normalized to those of untreated (control) samples. Absorbance readings were measured at 540 nm, using a SpectraMax M2^{e} Microplate Reader (Molecular Devices, Sunnyvale, CA) with SoftMax Pro software version 6.3 (Molecular Devices).

Flow Cytometric Analysis

Cell-cycle analysis was performed as previously described.[18] Briefly, cells were treated with indicated concentrations of ADI-PEG 20 for 48 hours, trypsinized, and fixed in 70% ethanol/30% phosphate-buffered saline v/v solution at 4°C. Signal acquisition was performed after staining with 20 μg/mL propidium iodide in phosphate-buffered saline containing 0.1% Triton X-100 and 100 μg/mL RNase for 30 minutes at room temperature. For analysis of apoptosis, cells were harvested, stained with propidium iodide and fluorescein isothiocyanate annexin V using the fluorescein isothiocyanate Annexin V Apoptosis Detection Kit I (BD Biosciences, San Jose, CA), and analyzed using a BD FACSCanto II flow cytometer with BD FACSDiva software version 6.1.3 (BD Biosciences).

Chloroquine Treatment and Immunofluorescence

Cells were treated with 25 μmol/L chloroquine (TCI America, Portland, OR) singly or in combination with ADI-PEG 20 at indicated concentrations for 6 hours and were subjected to Western blot analysis or immunofluorescence. For the latter, cells were plated on chamber slides (Nunc, Labtek, Thermo Scientific), treated as described, fixed in ice-cold 100% methanol, incubated with LC3A/B (dilution 1:200; Cell Signaling Technology), followed by anti-rabbit Alexa-conjugated secondary antibodies (Invitrogen, Carlsbad, CA), and mounted with Prolong Gold Antifade reagent with DAPI (Molecular Probes, Life Technologies).

Mouse Flank Xenograft Model and ADI-PEG 20 Administration

All studies were approved by the University of California, San Diego Institutional Animal Care and Use Committee. Six-week-old BALB/c nude/nude female mice (University

of California Animal Care Program) were injected with 1×10^6 cells in Matrigel (BD Biosciences) into the subcutaneous tissue of the flank. The left flank was injected with UM-UC-3 cells (ASS1-deficient), and the right flank was injected with RT112 cells (ASS1-expressor). Cells were allowed to grow for 8 days until a palpable nodule was present on each side; thereafter, the mice received once weekly intraperitoneal injections of saline (control mice) or 5 IU of ADI-PEG 20 dissolved in saline (drug-treated mice).[11–13] Tumors were measured every 4 days using vernier calipers (Thermo Fisher Scientific) by two authors (D.S. and K.N.), and the results were averaged. Tumor volumes were calculated using the formula: $0.5 \times$ (smaller dimension)$^2 \times$ (larger dimension). At the completion of the study, animals were euthanized using carbon dioxide asphyxiation, followed by bilateral thoracotomy. Tumors were excised, photographed, and formalin-fixed and paraffin-embedded. They were used to generate hematoxylin and eosin–stained slides for light microscopic analysis, Ki-67 immunostains (prediluted antibody; Ventana Medical Systems), and terminal deoxynucleotidyl transferase-mediated dUTP nick-end labeling (TUNEL) labeling using *in situ* Cell Death Detection Kit Fluorescein (Roche). The slides were mounted with Prolong Gold Antifade reagent with DAPI (Molecular Probes).

Data Extraction from TCGA

Data from the Cancer Genome Atlas Project (TCGA) project related to human bladder cancer were mined via the publically available University of California at Santa Cruz Cancer Genomics Browser,[19–21] and box plots of relative mRNA expression of the genes *ASS1* and *ASL* between tumor and normal tissue were obtained. Statistical analysis was performed within the browser using the Wilcoxon test option. Survival data from TCGA were obtained via the publically available cBioPortal[22,23] and was plotted on GraphPad Prism 5 (GraphPad Inc., San Diego, CA), with cases stratified according to mRNA expression either higher or lower than the median expression level, designated as high ASS1 and low ASS1, respectively.

Results

Loss of ASS1 Is Evident in Selected Subtypes of Bladder Cancer

We performed IHC to assess ASS1 protein expression in normal urothelium and invasive bladder cancers that included urothelial carcinoma, pure bladder adenocarcinoma, pure squamous cell carcinoma, and pure SCC. Normal urothelium demonstrated robust ASS1 expression throughout the full thickness of the urothelium by immunohistochemical analysis, whereas many invasive urothelial carcinomas and invasive squamous cell carcinomas of the bladder show reduced ASS1 expression (Figure 1A). Categories of invasive bladder cancer that showed a significant reduction in ASS1 expression compared with normal urothelium included urothelial carcinoma, SCC, and squamous cell carcinoma which had only 47.9% (71 of 148), 26.3% (5 of 19), and 10.2% (4 of 39) samples, respectively, that retained moderate-to-intense ASS1 expression (2+ or 3+ by IHC). In contrast, moderate-to-intense ASS1 expression (2+ or 3+ by IHC) was retained in 84.2% (16 of 19) of invasive bladder adenocarcinomas and 77.7% (21 of 27) of invasive micropapillary urothelial carcinomas, which represent an uncommon but aggressive subtype of urothelial carcinoma (Figure 1B). We next queried publicly available human bladder cancer data ($n = 426$) in TCGA database[24] using the University of California at Santa Cruz Cancer Genomics browser to assess relative mRNA expression of *ASS1* and *ASL* genes in normal bladder tissue and muscle-invasive bladder cancer. Relative mRNA expression of *ASS1* was significantly lower (Wilcoxon test; $P < 0.05$) in human bladder tumors than in normal tissue (Figure 1C). By contrast, *ASL* was significantly higher (Wilcoxon test; $P < 0.05$) in tumor samples than in normal tissue (Figure 1C). We analyzed the role of *ASS1* expression in affecting survival in this cohort of patients through cBioPortal ($n = 413$). Survival was significantly lower (log-rank and Gehan-Breslow-Wilcoxon tests; $P < 0.05$) in patients with low ASS1 expression than in patients with high ASS1 expression (Figure 1D).

ADI-PEG 20 Reduces Colony Formation and Cell Viability in ASS1-Deficient Bladder Cancer Cells

We identified by immunoblot analysis that the immortalized normal urothelial UROtsa cells and the invasive urothelial carcinoma-derived RT4, RT112, and 5637 bladder cancer cells retained ASS1 expression; several bladder cancer lines such as UM-UC-3, T24 and J82 cells expressed little to no ASS1 (Figure 1E). Jurkat cells were used as a positive control.[25] In colony formation growth assay performed with ADI-PEG 20 application over 6 to 11 days, ASS1-deficient UM-UC-3 and J82 cells formed few to no colonies when treated with ADI-PEG 20, whereas ASS1-expressing RT112 and 5637 bladder cancer cells formed colonies even in the presence of ADI-PEG 20, although colony number and size were diminished (Figure 2, A and B, and Supplemental Figure S1).

We next tested the effect of ADI-PEG 20 on cell viability with 48-hour application. Both J82 and UM-UC-3 cells, which showed reduced ASS1 protein expression, were growth inhibited by low ADI-PEG-20 concentrations [concentration that inhibits 50% (IC_{50}) of 0.1 and 0.34 μg/mL and area under the curve (AUC) of 13.7 and 33.69 for J82 and UM-UC-3 cells, respectively] (Figure 2, C–E). In contrast, RT112 cells, which expressed the most ASS1 protein by immunoblot, demonstrated little cell death on exposure to ADI-PEG-20 ($IC_{50} > 1.2$ μg/mL, AUC of 77) (Figure 2, C and F). The 5637 cells, which expressed an

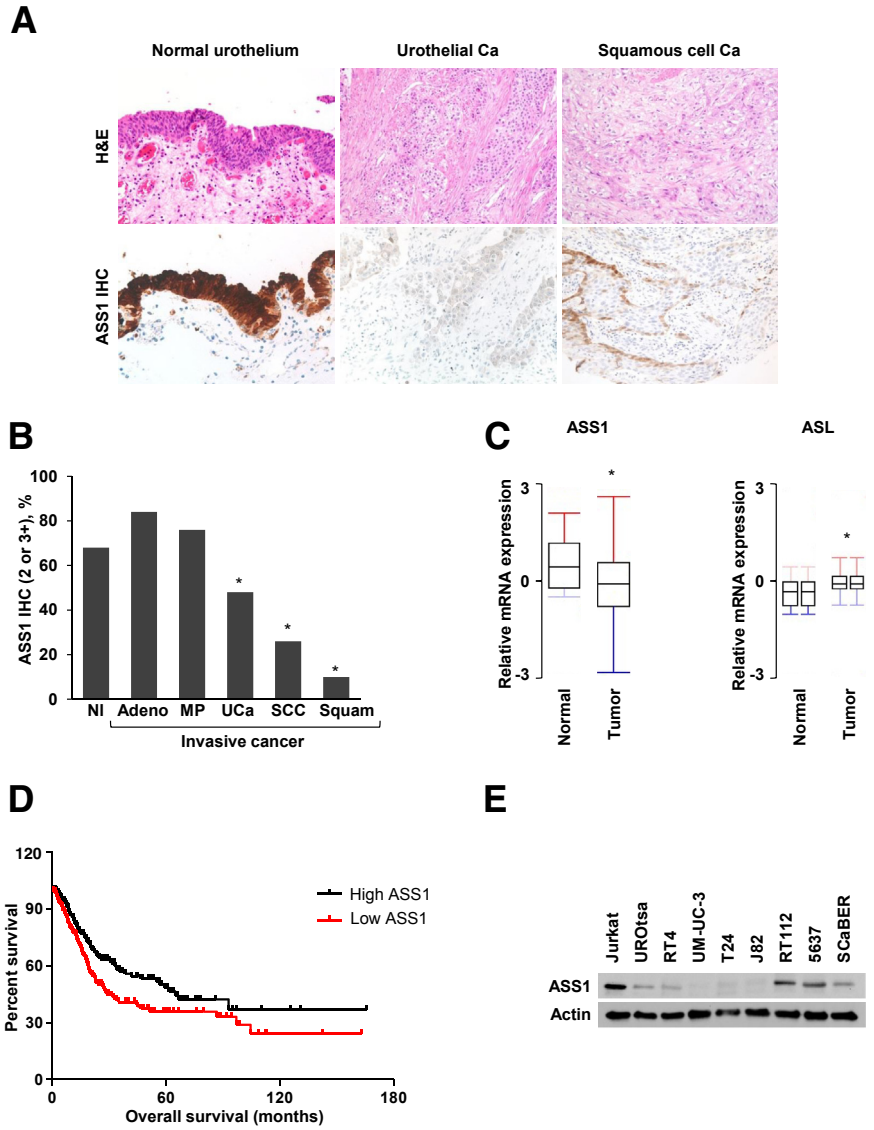

Figure 1 ASS1 expression is reduced in some human bladder cancers and cell lines. **A:** Normal urothelium, urothelial carcinoma, and squamous cell carcinoma were assessed for ASS1 expression by immunohistochemistry. **B:** The percentage of cells showing 0 or 1+ ASS1 expression (on a scale of 0–3) is shown for a series of Nl and invasive carcinomas, consisting of Adeno, MP, UCa, SCC, and Squam. **C:** Box plots representing relative mRNA expression levels of *ASS1* and *ASL* in human bladder tumors compared with normal, from the TCGA database. The data for *ASL* were split into two subcolumns because two probes map onto the same gene. **D:** Overall patient survival plotted related to ASS1 expression; high ASS1 (above median) versus low ASS1 (below median). **E:** Representative immunoblot of ASS1 in benign and malignant bladder cells; Jurkat cells were used as a positive control. $n = 19$ Nl (**B**); $n = 19$ Adeno (**B**); $n = 27$ MP (**B**); $n = 148$ UCa (**B**); $n = 19$ SCC (**B**); $n = 39$ Squam (**B**). $^*P < 0.05$ compared with normal urothelium, Fishers test (**B**); $^*P < 0.05$ compared with normal, Wilcoxon test (**C**); $P = 0.0082$, log-rank (Mantel Cox) text, $P = 0.0072$, Gehan-Breslow-Wilcoxon text (**D**). Original magnification, ×100 (**A**). Adeno, adenocarcinoma; ASL, argininosuccinate lyase; ASS1, argininosuccinate synthetase 1; Ca, carcinoma; H&E, hematoxylin and eosin; IHC, immunohistochemistry; MP, micropapillary urothelial carcinoma; Nl, normal urothelium; SCC, small cell carcinoma; Squam, squamous cell carcinoma; TCGA, the Cancer Genome Atlas Project; UCa, urothelial carcinoma.

intermediate amount of ASS1 protein, showed intermediate sensitivity to ADI-PEG-20 (IC_{50} of 0.27 μg/mL, AUC of 51.3) (Figure 2, C and G).

To test if J82 and UM-UC-3 cells functioned as arginine auxotrophs, we cultured these cells in the presence of the arginine precursor citrulline and concurrently treated these cells with ADI-PEG 20. Citrulline was unable to rescue the cells from arginine deprivation caused by ADI-PEG 20 (Supplemental Figure S2), indicating that the cells are unable to synthesize arginine endogenously to compensate for microenvironmental depletion.

ADI-PEG 20 Induces Caspase-Independent Apoptosis and Autophagy in ASS1-Deficient Bladder Cancer Cells

To study the mechanism whereby ADI-PEG 20 induces cell death, we performed propidium iodide cell-cycle analysis in ASS1-expressing and ASS1-deficient bladder cancer cells after ADI-PEG 20 treatment for 48 hours. A dose-dependent increase in the sub-G1 fraction was demonstrated with ADI-PEG 20 in ASS1-deficient UM-UC-3 cells (3.7% sub-G1 fraction in untreated versus 31.9% sub-G1 fraction with 1.2 μg/mL ADI-PEG 20 treatment). A similar effect was seen in ASS1-deficient J82 cells. However, ASS1-expressing RT112 and 5637 cells did not show a shift to a sub-G1 fraction on applying ADI-PEG 20 (Figure 3A and Supplemental Figure S3A). We next used fluorescence-activated cell sorting analysis to verify that the sub-G1 population represented apoptotic cells, which were detected as the sum of early apoptotic (annexin V–positive and propidium iodide–negative) and late apoptotic (annexin V and propidium iodide double positive) cells (Figure 3, B and C, and Supplemental Figure S3B).

Consistent with our fluorescence-activated cell sorting analysis results, we found that 48 hours of treatment with ADI-PEG 20 induced PARP cleavage in ASS1-deficient cells

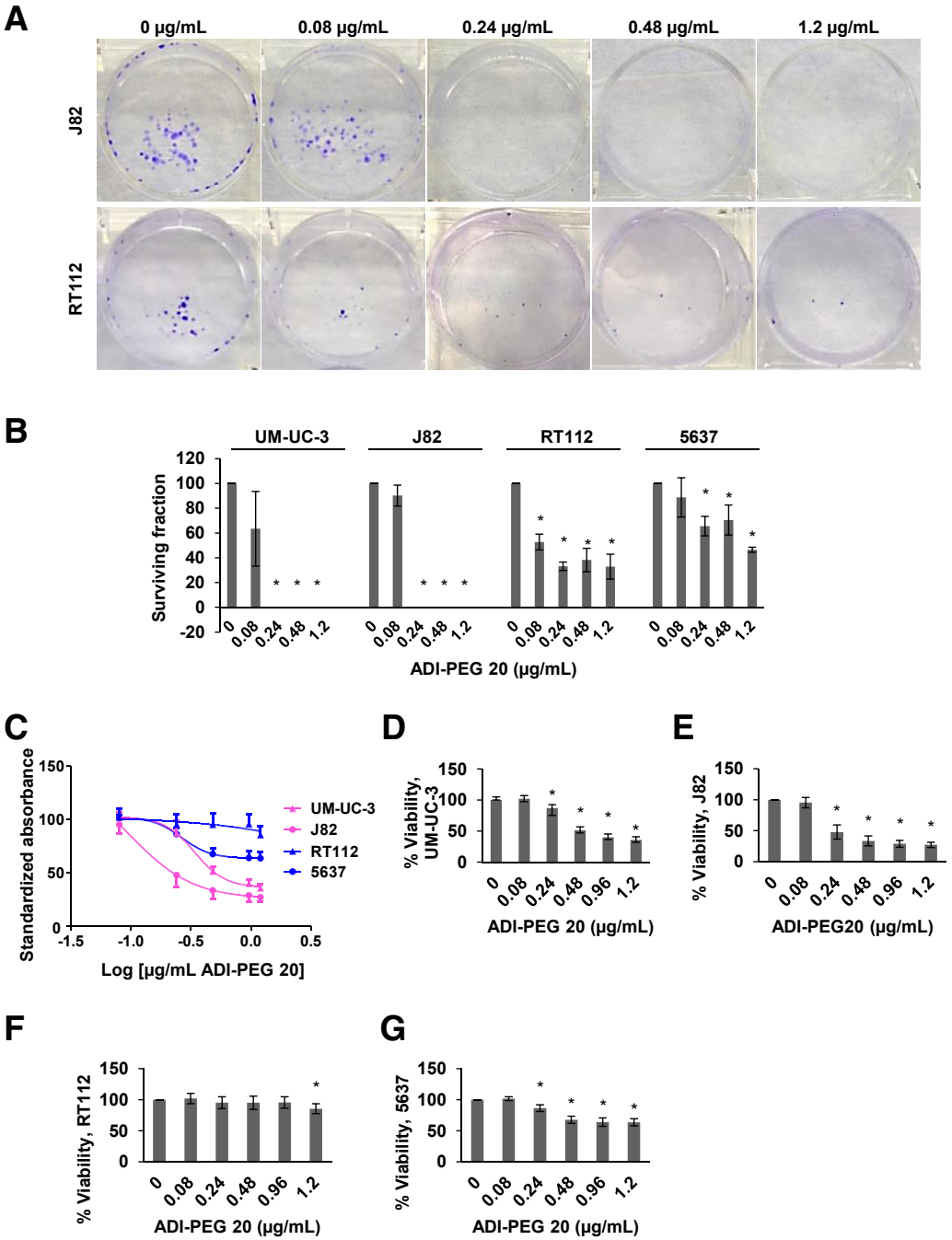

Figure 2 ADI-PEG 20 reduces colony formation growth and cell viability in ASS1-deficient bladder cancer cells. **A:** Representative images are shown for colony formation in J82 and RT112 cells treated with increasing concentrations of ADI-PEG 20 for 6 to 10 days. **B:** Quantification of surviving fraction of colonies from colony formation assays in UM-UC-3, J82, RT112, and 5637 cells. **C:** Results from three independent MTT assays to calculate IC_{50} and AUC. **D**–**G:** Cell viability in UM-UC-3, J82, RT112, and 5637 cells, respectively, treated with increasing concentrations of ADI-PEG 20 for 48 hours. $^*P < 0.05$ compared with untreated control, *t*-test. ADI-PEG 20, pegylated arginine deiminase; ASS1, argininosuccinate synthetase 1; AUC, area under the curve; IC_{50}, concentration that inhibits 50%.

but not in ASS1-expressing cells (Figure 3, D and E, and Supplemental Figure S3, C and D). The apoptosis and PARP cleavage induced by ADI-PEG 20 likely occurs via a caspase-independent mechanism, because we found no evidence of caspase 3, 7, or 9 cleavage in ADI-PEG 20–treated cells (Figure 3, D and E, and Supplemental Figure S3, C and D).

ADI-PEG 20 can elicit autophagy in some tumor types,[7] which may be assayed by increased conversion of LC3I to LC3II. We identified that treatment with both increasing concentrations of ADI-PEG 20 as well as arginine-free culture medium for 6 hours could increase the conversion of LC3I to LC3II, in ASS1-deficient UM-UC-3 and J82 cells compared

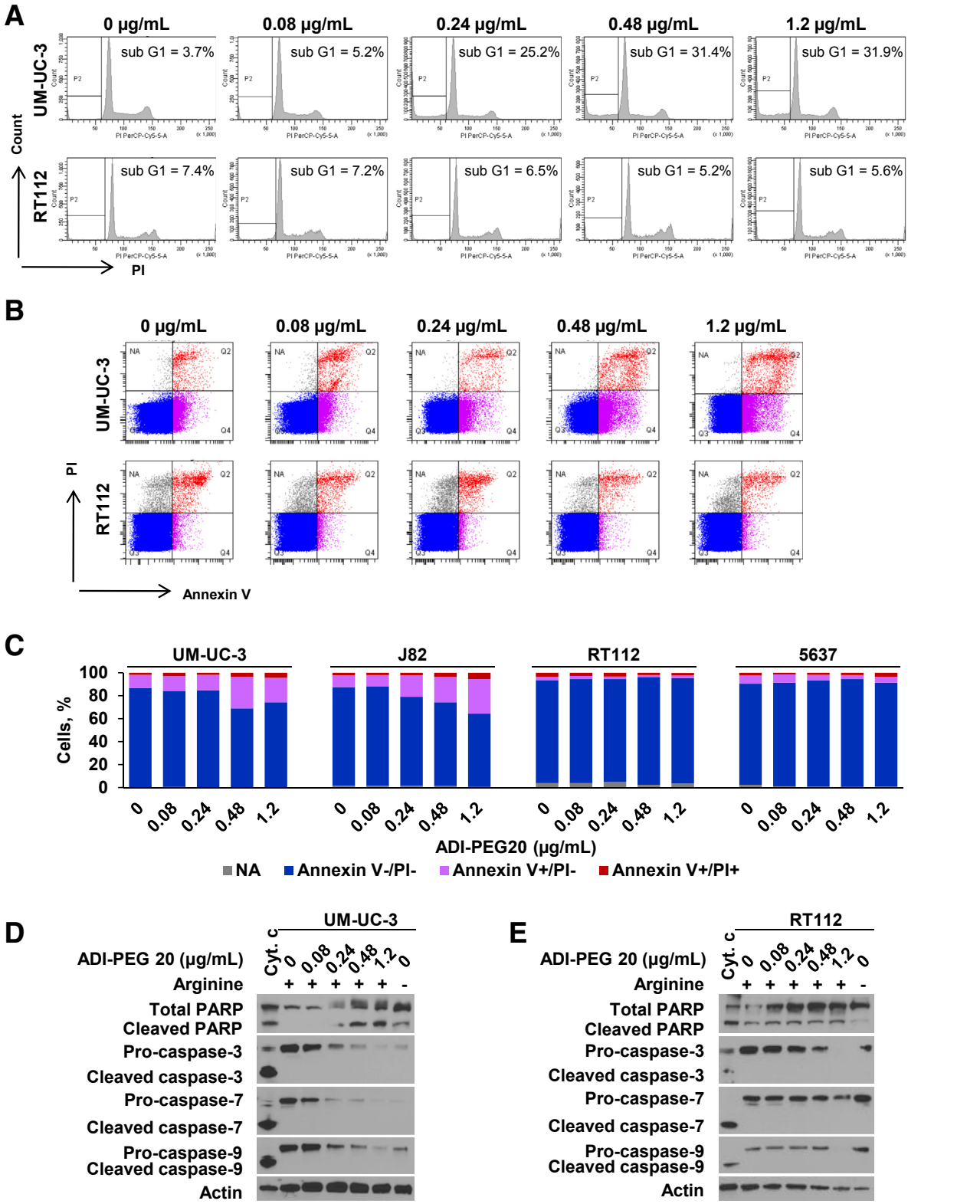

Figure 3 Arginine deprivation therapy leads to caspase-independent apoptotic cell death in ASS1-deficient cells. **A:** PI-based cell-cycle analysis in UM-UC-3 and RT112 cells treated with increasing concentrations of ADI-PEG 20 for 48 hours. **B:** PI/annexin V flow cytometric analysis in UM-UC-3 and RT112 cells treated with increasing concentrations of ADI-PEG 20 for 48 hours. **C:** Quantification of PI/annexin V flow cytometric analysis of UM-UC-3, J82, RT112, and 5637 bladder cancer cells. **D** and **E:** Immunoblot of PARP and caspase cleavage in ASS1-deficient and -expressing cell lines treated with increasing concentrations of ADI-PEG 20 for 48 hours. Cytochrome C lysate was used as positive control. Data from a single experiment, representative of three independent experiments are presented (**B**). ADI-PEG 20, pegylated arginine deiminase; ASS1, argininosuccinate synthetase 1; Cyt C, cytochrome C; PARP, poly (ADP-ribose) polymerase; NA, not applicable; PI, propidium iodide.

with untreated cells (Figure 4A). ASS1-expressing RT112 and 5637 cells did not show this response. The autophagy inhibitor chloroquine also increased LC3II accumulation, and this effect was enhanced on co-treatment with ADI-PEG 20 in ASS1-deficient cells but not in ASS1-expressing cells (Figure 4A). Thus, ADI-PEG 20 appears to increase autophagy in ASS1-deficient bladder cancer cells. Finally, in support of this result, we observed an increase in LC3-positive punctae by immunofluorescence in UM-UC-3 and J82 cells after either ADI-PEG 20 or chloroquine treatment (Figure 4B). This finding has been associated with a redistribution of LC3 to autophagosomes and an increase in autophagy.[12] The greatest increase in punctae occurred with co-incubation with both drugs.

ADI-PEG 20 Induces GCN2-Dependent eIF2α Phosphorylation (Ser51) and ATF4-CHOP Induction in ASS1-Deficient Bladder Cancer Cells

Because arginine deprivation can cause cell stress, we evaluated the effects of arginine deprivation and ADI-PEG 20 application on expression and activity of eIF2. eIF2 is an environmental stress response protein that mediates growth arrest and apoptosis through downstream transcriptional regulators as part of the amino acid response pathway,[26] including ATF4 and CHOP.[27,28] ADI-PEG 20 application for 6 hours induced p-eIF2α in ASS1-deficient UM-UC-3 and J82 cells, slightly in RT112 cells, and none in 5637 cells. It led to expression of both ATF4 and CHOP in ASS1-deficient UM-UC-3 and J82 cells but not in ASS1-expressing RT112 and 5637 cells (Figure 5A). Complete arginine deprivation using arginine-free media resulted in variable elevation of eIF2α phosphorylation and ATF4 and CHOP expression in all cells (Figure 5A).

Modulation of ASS1 Expression by Overexpression/Silencing Reverses Response to ADI-PEG 20 in ASS1-Deficient/Expressing Bladder Cancer Cells

To test the correlation between ASS1 expression and sensitivity to ADI-PEG 20, we overexpressed ASS1 in ASS1-deficient UM-UC-3 cells (Figure 5B) and used siRNA to silence ASS1 in ASS1-expressing RT112 cells (Figure 5C). ASS1-overexpressing UM-UC-3 cells showed less growth inhibition by ADI-PEG 20, compared with empty vector—transfected control cells; in contrast, RT112 transfected with ASS1-targeting siRNA showed greater growth inhibition by ADI-PEG 20 than cells transfected with

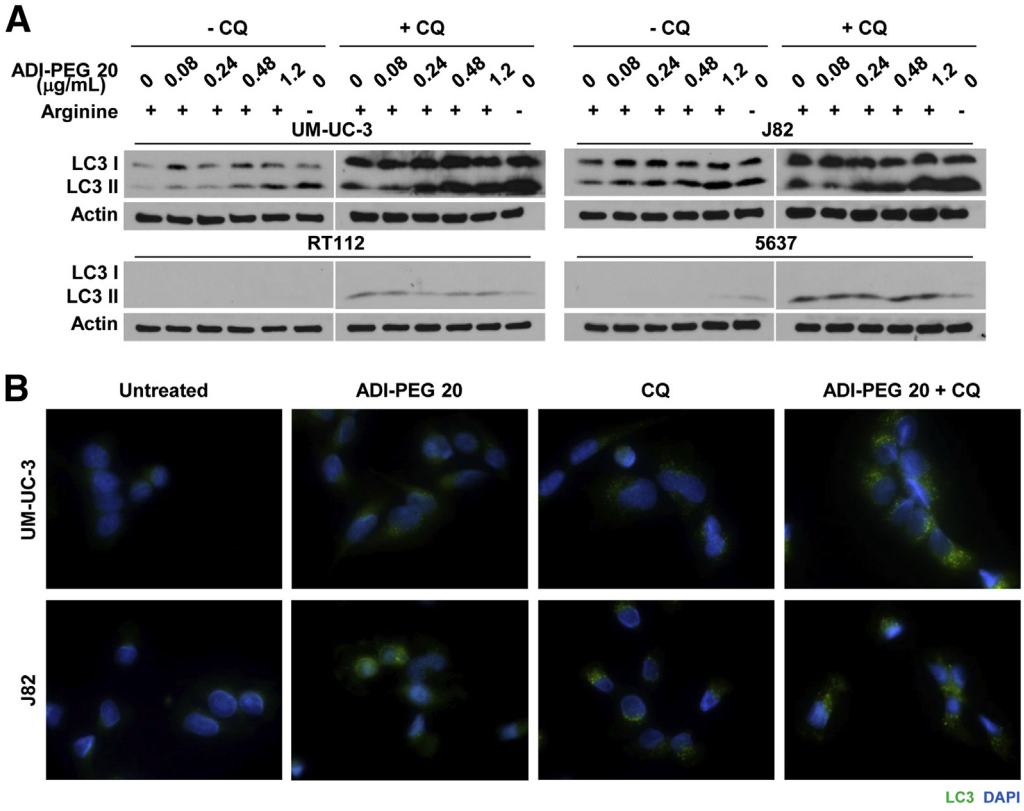

Figure 4 Arginine deprivation or ADI-PEG 20 treatment leads to autophagy in ASS1-deficient bladder cancer cells. **A:** Representative immunoblots of LC3I and LC3II in UM-UC-3, J82, RT112, and 5637 cells after ADI-PEG 20 administration alone, or with CQ, for 6 hours. Arginine-free media were used as arginine deprivation control. **B:** LC3 punctae were increased in UM-UC-3 and J82 cells on ADI-PEG 20 or CQ treatment for 6 hours, compared with untreated cells. Co-incubation of cells with both ADI-PEG 20 and CQ caused the greatest increase in punctae. DAPI was used to counterstain the nucleus. ADI-PEG 20, pegylated arginine deiminase; ASS1, argininosuccinate synthetase 1; CQ, chloroquine.

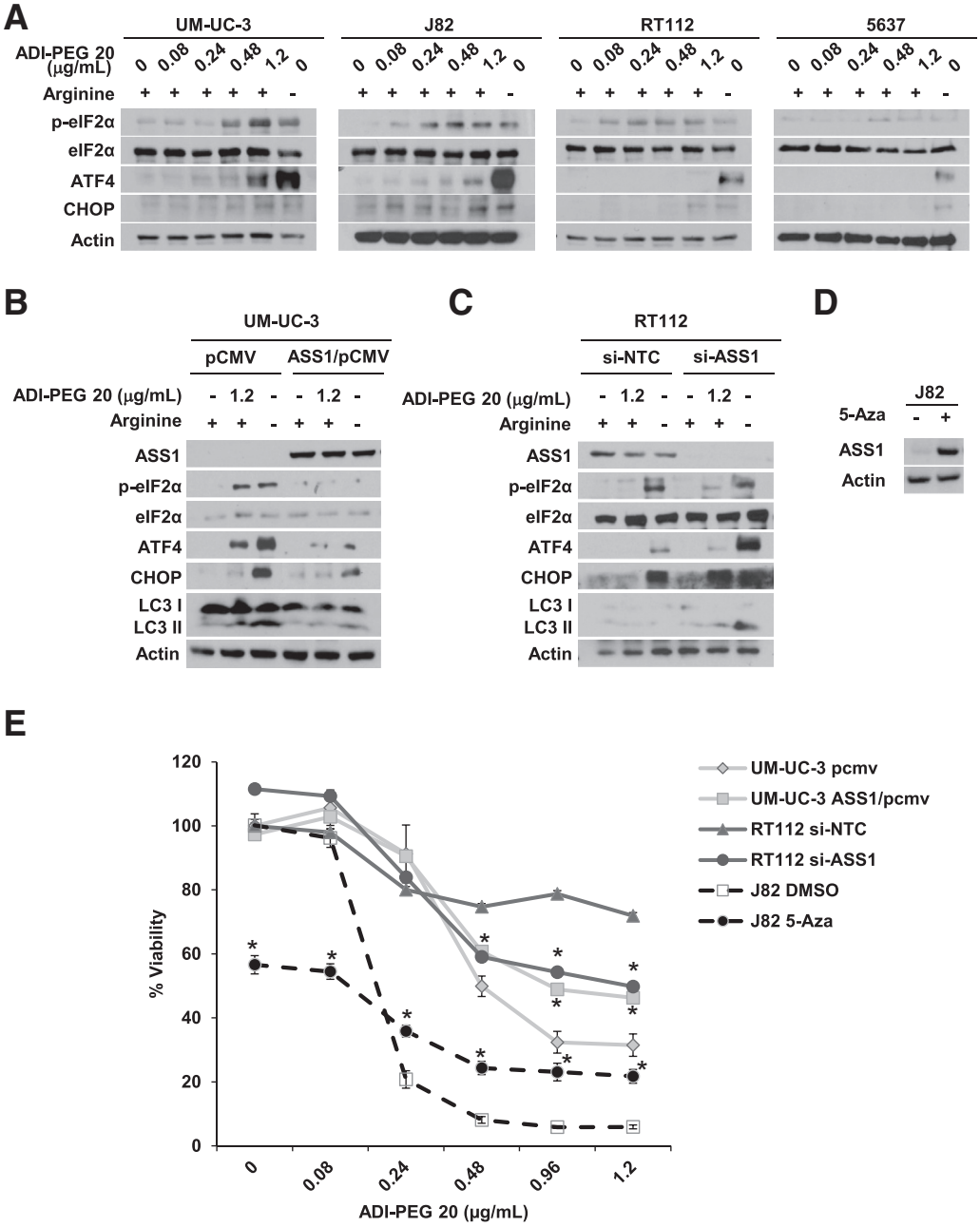

Figure 5 Arginine deprivation or ADI-PEG 20 treatment leads to eIF2α phosphorylation (Ser51), ATF4-CHOP induction, and LC3II accumulation in ASS1-deficient bladder cancer cells. **A:** Immunoblot of p-eIF2α (Ser51), ATF4, and CHOP in UM-UC-3, J82, RT112 and 5637 cells after ADI-PEG 20 administration for 6 hours. Arginine-free media were used as arginine deprivation control. **B** and **C:** p-eIF2α (Ser51), ATF4, and CHOP induction, and LC3II accumulation on treatment with ADI-PEG 20 or arginine-free media for 6 hours is ablated in ASS1-overexpressing UM-UC-3 cells compared with empty vector control cells (**B**) and increased in ASS1-silenced RT112 cells compared with NTC control cells (**C**). **D:** Immunoblot of ASS1 shows re-expression in J82 cells on 5-Aza treatment. **E:** MTT assays in the aforementioned cells for 48 hours. $*P < 0.05$ compared with respective controls (UM-UC-3 pCMV, RT112 si-NTC, or J82 DMSO) at each ADI-PEG 20 concentration, *t*-test. ADI-PEG 20, pegylated arginine deiminase; ASS1, argininosuccinate synthetase 1; ATF4, activating transcription factor 4; CHOP, C/EBP homologous protein; DMSO, dimethyl sulfoxide; eIF2α, eukaryotic initiation factor 2α; pCMV, cytomegalovirus plasmid; p-eIF2α, phosphorylated eukaryotic initiation factor 2α; si-NTC, nontargeting control siRNA; 5-Aza, 5-azacytidine.

NTC siRNA (Figure 5E). Methylation of the ASS1 promoter represses *ASS1* gene expression,[4] and we found that the demethylating agent 5-Aza induced ASS1 expression in ASS1-deficient J82 cells (Figure 5D). 5-Aza also decreased the sensitivity of the cells to ADI-PEG 20 compared with DMSO-treated control cells (Figure 5E). We observed decreased viability in cells treated with 5-Aza alone, which can be because it is a nonspecific global demethylating agent that can affect numerous pathways as well as cause DNA damage, both of which can lead to decrease in viability.

We also found increased conversion of LC3I to LC3II on 6 hours of treatment with ADI-PEG 20 or arginine-free media in empty vector—transfected UM-UC-3 cells, which was decreased in ASS1-overexpressing cells (Figure 5B and Supplemental Figure S4A). In contrast, RT112 cells containing ASS1-targeting siRNA showed greater conversion of LC3I to LC3II when incubated with ADI-PEG 20 or arginine-free media compared with cells transfected with NTC siRNA (Figure 5C and Supplemental Figure S4B). ASS1 overexpression in ASS1-deficient UM-UC-3 cells ablated ADI-PEG 20 application-induced p-eIF2α and expression of both ATF4 and CHOP (Figure 5B), whereas ASS1-silenced RT112 cells showed ATF4, CHOP, and p-eIF2α expression (Figure 5C).

eIF2α Phosphorylation (Ser51) and CHOP Induction after ADI-PEG 20 Treatment Is Due to GCN2 Kinase Activation

Reduced tRNA charging in response to amino acid deprivation is regulated by GCN2 kinase. We evaluated if GCN2 kinase expression contributed to elevated eIF2α phosphorylation in response to arginine deprivation in ASS1-deficient cells. Whereas transfection of the ASS1-deficient J82 and UM-UC-3 cells with NTC siRNA caused an increase in eIF2α phosphorylation and ATF4 and CHOP expression after 6 hours of incubation in ADI-PEG 20 or arginine-free media, these changes were ablated when GCN2 was selectively silenced (GCN2-siRNA) (Figure 6A). Separate experiments in which ATF4 or CHOP was silenced in UM-UC-3 cells were performed. ATF4-silenced cells showed a slight increase in eIF2α phosphorylation in response to incubation in ADI-PEG 20 or arginine-free media for 6 hours but no expression of ATF4 and CHOP. CHOP-silenced cells showed no induction of eIF2α phosphorylation and modest ATF4 expression on ADI-PEG 20 treatment, whereas arginine-free media caused no induction of eIF2α phosphorylation but induction of ATF4 expression. Both treatments did not induce CHOP. This suggests a possible feedback mechanism (Figure 6B). The GCN2-ATF4-CHOP pathway has been reported to control autophagy,[27] and we observed reduced autophagy in GCN2-, ATF4-, or CHOP-silenced cells with incubation of ASS1-deficient cells in ADI-PEG 20 or arginine-free media, as evident from decreased LC3II to LC3I ratios (Figure 6, A—D). A summary of this pathway is presented in Figure 6E.

ADI-PEG 20 Administration Reduces Tumor Growth *in Vivo*

We next assessed the effect of ADI-PEG 20 on tumor growth *in vivo*. We inoculated nude mice with ASS1-expressing RT112 cells and ASS1-deficient UM-UC-3 cells into the subcutaneous tissue on opposite flanks of the same animal. When tumors reached a palpable size (average 40 mm^3 after 8 days), we initiated weekly intraperitoneal injections of either 5 IU of ADI-PEG 20 or an equivalent volume of saline for 3 weeks, based on optimal concentrations from previous studies.[11—13] No statistically significant difference in tumor size was noted between control and treatment groups at initiation of treatment (*t*-test; $P > 0.05$). Mice treated with ADI-PEG 20 showed a marked decrease in ASS1-deficient UM-UC-3 tumor growth, in contrast to saline control animals (*t*-test; $P < 0.05$) (Figure 7A). Contralateral ASS1-expressing RT112 tumors showed only a minor and nonsignificant trend toward reduced tumor volumes when treated with ADI-PEG 20 (*t*-test; $P > 0.05$). Differences in tumor size were evident on both external examination (Figure 7B) and in dissected tissue (Figure 7C). Histologic review of mouse xenografts showed that UM-UC-3 tumors treated with ADI-PEG 20 had a reduction in tumor cell number, a 90% reduction in Ki-67 proliferation index relative to saline-treated tumors (*t*-test; $P < 0.05$), and a 60% increase in TUNEL labeling relative to saline-treated tumors (*t*-test; $P < 0.05$) (Figure 7, D—F).

Discussion

Despite the high incidence of bladder cancer, limited options for targeted treatment are available for this patient population. We evaluated the potential of ADI-PEG 20, which degrades extracellular arginine and reduces cell growth in ASS1-deficient cells, as a potential new targeted therapy in bladder cancer. Although ADI-PEG 20 is effective against various ASS1-deficient tumor cell types *in vitro* and is currently in clinical trials for melanoma and hepatocellular carcinoma,[4,8,9,14] its role in bladder cancer requires further investigation.

We evaluated ASS1 expression in normal urothelium and invasive human bladder cancers, including urothelial carcinoma, pure squamous cell carcinoma, pure adenocarcinoma, and pure SCC. Conventional urothelial carcinoma, SCC, and squamous cell carcinoma subtypes of bladder cancer all showed significantly reduced levels of ASS1 compared with normal urothelium. This finding suggests that these three major subtypes of bladder cancer, which account for >90% of all bladder cancers, may potentially respond to ADI-PEG 20. Furthermore, limited alternative therapies have been historically available for either SCC or squamous cell carcinoma of the bladder, further highlighting the importance of ASS1 loss and the actionable role of ADI-PEG 20 in this scenario. Although one prior study has also shown an association between ASS1 reduction and decreased survival in bladder cancer patients,[29] the grade and stage of the patients included for study were not specified. We specifically focused our analysis on the association between ASS1 loss and survival using a large publicly available data set of invasive urothelial carcinoma and show that ASS1 loss may also be a putative prognostic factor in this bladder cancer group. Future studies that address in depth the association

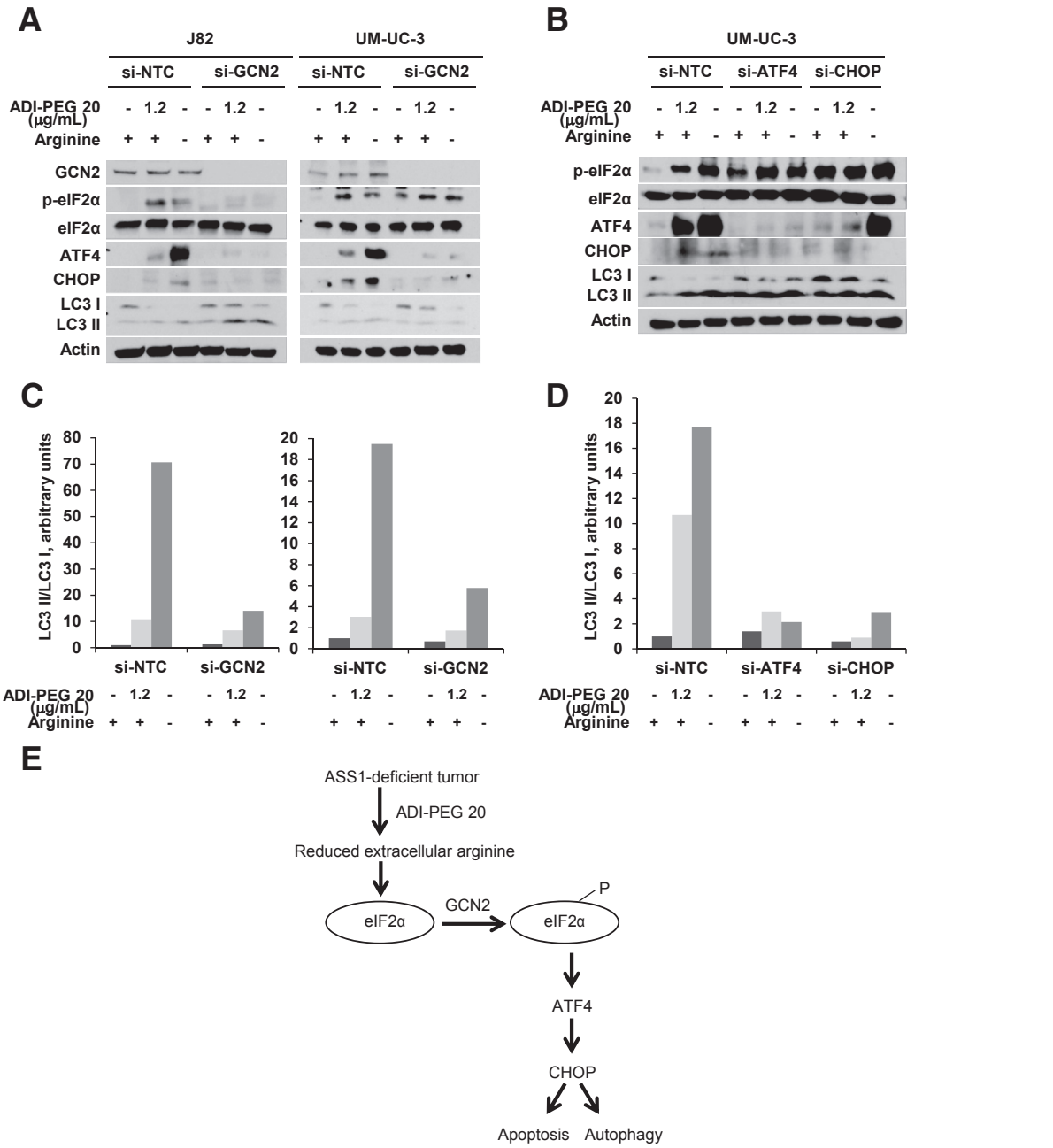

Figure 6 Arginine deprivation or ADI-PEG 20 treatment leads to GCN2 kinase-mediated eIF2α phosphorylation (Ser51) in ASS1-deficient bladder cancer cells. **A:** J82 and UM-UC-3 cells were transfected with NTC-siRNA or GCN2-siRNA and effects on eIF2α (Ser51) phosphorylation, ATF4, CHOP, and LC3 was assessed after ADI-PEG20 or arginine-free media administration for 6 hours. **B:** UM-UC-3 cells were transfected with control (NTC) siRNA, ATF4-siRNA, or CHOP-siRNA, and effects on eIF2α (Ser51) phosphorylation, ATF4, CHOP, and LC3 were assessed after ADI-PEG20 or arginine-free media administration for 6 hours. **C** and **D:** LC3II/LC3I ratios in the above figures plotted by densitometry. **E:** Schematic of putative drug mechanism in ASS1-deficient bladder cancer cells treated with ADI-PEG 20. ADI-PEG 20, pegylated arginine deiminase; ASS1, argininosuccinate synthetase 1; ATF4, activating transcription factor 4; CHOP, C/EBP homologous protein; eIF2α, eukaryotic initiation factor 2α; GCN2, general control nonderepressible 2; NTC, nontargeting control.

between ASS1 expression and nonmuscle invasive bladder cancer could potentially expand the spectrum of ADI-PEG 20—targetable bladder cancers and better delineate the onset of ASS1 loss during bladder cancer progression. The loss of ASS1 by DNA methylation has been reported,[29] and we have confirmed this in our invasive bladder cancer cell lines. An additional mechanism of ASS1 loss in human bladder cancers may be due to loss of chromosome 9q which contains ASS1.[30]

ADI-PEG 20 selectively targets ASS1-deficient cells by degradation of arginine in the extracellular milieu, thereby inducing cell death in ASS1-deficient arginine auxotrophs. We focused our *in vitro* assays on the urothelial carcinoma subtype of bladder cancer, which represents most bladder

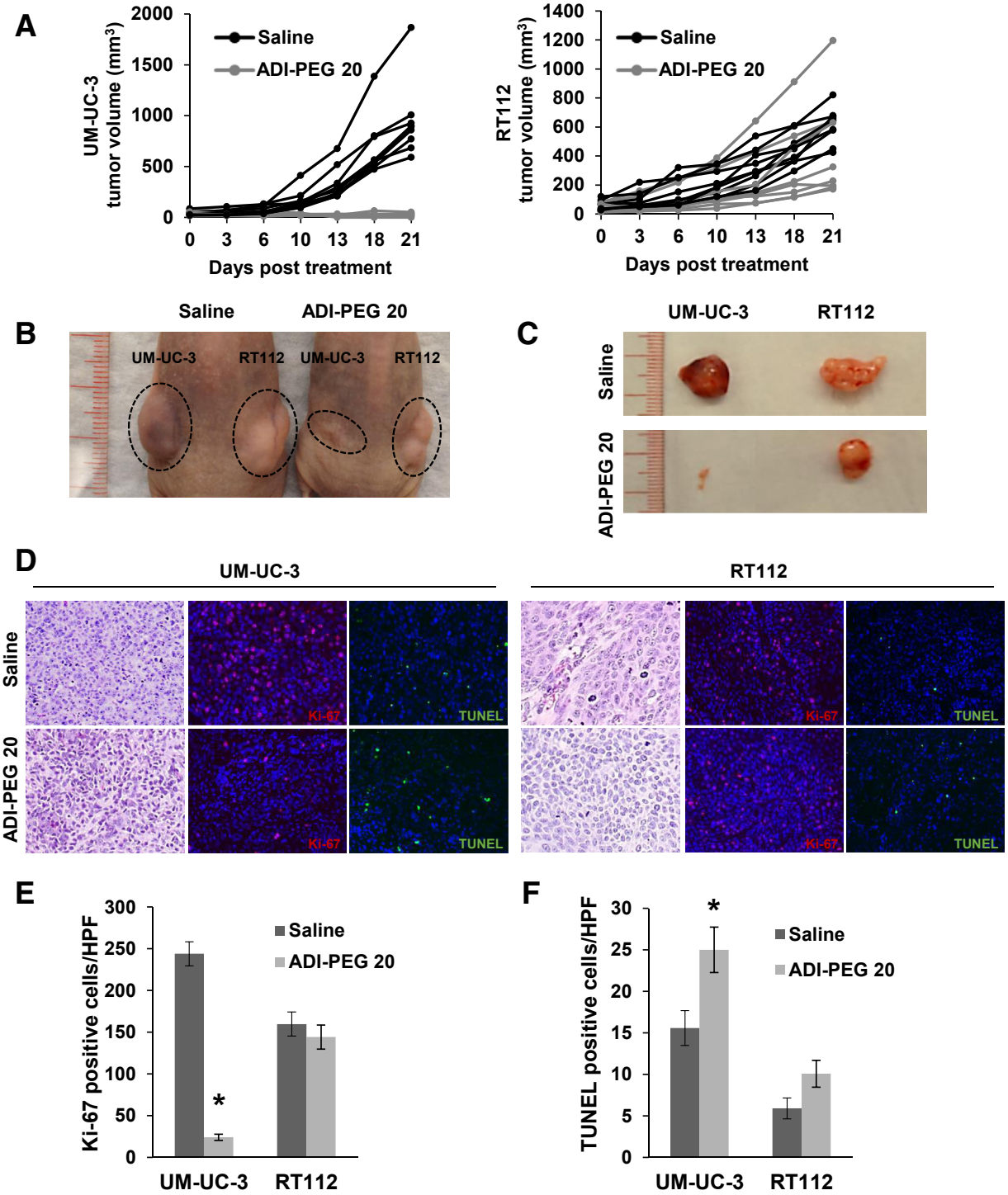

Figure 7 ASS1 deficiency results in reduced tumor growth in a xenograft model of bladder cancer. **A:** Athymic nude mice containing UM-UC-3 xenografts (left flank) and RT112 xenografts (right flank) showed reduced UM-UC-3 volume after ADI-PEG 20 administration. **B:** Image of mouse xenografts after treatment with saline or ADI-PEG20. **C:** Grossly dissected mouse tumors after saline and ADI-PEG 20 treatment. **D:** H&E staining showed reduced cell numbers in ADI-PEG 20—treated tumors that correlated with reduced Ki-67 proliferation index and increased TUNEL stain. **E:** Quantification of Ki-67 staining. **F:** Quantification of TUNEL staining. $*P < 0.05$, *t*-test. Original magnification, ×20 (**D**). ADI-PEG 20, pegylated arginine deiminase; ASS1, argininosuccinate synthetase 1; H&E, hematoxylin and eosin; TUNEL, terminal deoxynucleotidyl transferase-mediated dUTP nick-end labeling.

cancer cases and which has numerous cell lines available for *in vitro* analysis, in contrast to the other major subtypes of bladder cancer. Several bladder cancer cell lines, including J82, UM-UC-3, and T24, showed loss of ASS1 expression. In comparison with ASS1-expressing bladder cancer cell lines, ASS1-deficient bladder cancer cells showed a significant increase in sensitivity to ADI-PEG 20 application. Specifically, a dose-dependent reduction in colony

formation and cell survival were seen in ASS1-deficient cell lines after ADI-PEG 20 application. Cell death secondary to ADI-PEG 20 administration in ASS1-deficient cells was accompanied by a significant increase in the sub-G1 fraction that was associated with caspase-independent apoptosis. This result is consistent with that of a prior study, which showed caspase-independent apoptotic cell death in ADI-PEG 20–treated prostate cancer cells[12]; however, other studies in different cancer types have shown caspase-dependent mechanisms of cell death after ADI-PEG 20 application.[11] This suggests that the downstream apoptotic mechanism in response to ADI-PEG 20 may be cell-type specific. We expanded the analysis on cell death to include testing of LC3I to LC3II conversion and analysis of LC3II accumulation, suggesting that autophagy may occur in association with apoptotic cell death in the context of ADI-PEG 20 application.

We further investigated the signaling mechanism responsible for apoptosis in ASS1-deficient bladder cancer cells after ADI-PEG 20 administration. ADI-PEG 20 increased phosphorylation of the regulatory subunit of eIF2, a stress-response protein activated during amino acid deprivation,[27] which activates the amino acid response pathway. Increased eIF2 activity has been shown to decrease translation of most mRNAs but stimulates selected translation pathways containing genes having the amino acid response element,[26] such as increase in translation of the ATF4 transcription factor and its downstream pro-apoptotic target CHOP.[28] Upstream regulation of eIF2 can be influenced by a number of proteins, including GCN2, protein kinase double-stranded RNA-activated, protein kinase double-stranded RNA activated–like endoplasmic reticulum kinase, and heme-regulated inhibitor.[31–34] We selectively tested the role of GCN2, which couples amino acid starvation to the eIF-ATF4 pathway and regulates eIF2 phosphorylation,[27,35] as a potential mediator of eIF2α phosphorylation and apoptosis in the context of arginine auxotrophic bladder cancer cells. The results from our study suggest that the GCN2-ATF4-CHOP pathway can regulate autophagy during arginine deprivation in ASS1-deficient bladder cancer cells. This also suggests the potential to couple ADI-PEG 20 therapy with other mediators of the cell stress response, such as the mammalian target of rapamycin pathway,[36] which has been shown to be critical to bladder cancer cell proliferation and survival.[17]

To validate our results in a xenograft model, we used dual inoculation of RT112 and UM-UC-3 cells on contralateral mouse flanks to test the effects of intraperitoneal ADI-PEG 20 administration on differential growth of ASS1-deficient and ASS1-expressing bladder cancer cell lines. ADI-PEG 20 arrested bladder cancer cell growth selectively in ASS1-deficient cells. These ASS1-deficient xenograft tumors showed tumor cell dropout, markedly reduced Ki-67 proliferation rates, and increased apoptosis that likely account for reduced tumor volumes and that are consistent with other studies in different cancer types.[11–14] We used a single concentration to test the effects of ADI-PEG 20 administration on bladder cancer growth; however, future studies that expand the therapeutic range of ADI-PEG 20 could refine dosing of this drug. One interesting finding is that a subset of ASS1-expressing RT112 xenografted bladder tumors showed a partial response to ADI-PEG 20 administration. Although we have not tested the mechanism underlying this partial response, one possibility is that severe arginine depletion in the context of high-dose ADI-PEG 20 administration may result in nonspecific metabolic cell stress and a reduction in cell growth in ASS1-expressing cells, similar to what was noted in the colony formation assay. In such an instance, however, one potential means to enhance ADI-PEG 20 effect may be to combine this treatment with chemotherapy to stress partial arginine auxotrophs and to enhance response rate.[2] This strategy is currently being used in several studies in which ADI-PEG 20 is being used in combination with single or multiple chemotherapy in other cancer types (*https://clinicaltrials.gov*, identifiers NCT01497925, NCT02029690, NCT02101593, NCT02102022, NCT02101580, NCT02006030, NCT01-948843, NCT01665183, and more that are not currently active).

There is a major unmet need to identify additional therapies for bladder cancer patients that include agents that can target both conventional urothelial carcinoma and less common subtypes of bladder cancer. We identified ASS1 loss in a large proportion of bladder cancers and showed that ASS1-deficient bladder cancer cells undergo apoptosis in response to ADI-PEG 20 *in vitro* and *in vivo*. These findings suggest that arginine dependency in bladder cancer may be a useful mechanism to selectively target a subset of these cancers using ADI-PEG 20, although further investigation into the mediators of this effect and the role of combination therapy to enhance efficacy is required. In addition, expansion of these studies to include patients with non-muscle invasive bladder cancer may be of value in determining whether systemic or intravesical ADI-PEG 20 administration could be a novel therapeutic approach in this setting. Finally, the results from this study suggest that arginine-derived metabolites may be important in bladder cancer growth and survival and are of interest in future studies of this disease.

Acknowledgments

We thank Dr. Donald Pizzo and the University of California at San Diego Pathology Tissue Technology Core for conducting the hematoxylin and eosin and Ki-67 staining on mouse xenograft sections.

Supplemental Data

Supplemental material for this article can be found at *http://dx.doi.org/10.1016/j.ajpath.2016.09.004*.

References

1. Tennant DA, Duran RV, Gottlieb E: Targeting metabolic transformation for cancer therapy. Nat Rev Cancer 2010, 10:267−277
2. Phillips MM, Sheaff MT, Szlosarek PW: Targeting arginine-dependent cancers with arginine-degrading enzymes: opportunities and challenges. Cancer Res Treat 2013, 45:251−262
3. Haines RJ, Pendleton LC, Eichler DC: Argininosuccinate synthase: at the center of arginine metabolism. Int J Biochem Mol Biol 2011, 2: 8−23
4. Delage B, Luong P, Maharaj L, O'Riain C, Syed N, Crook T, Hatzimichael E, Papoudou-Bai A, Mitchell TJ, Whittaker SJ, Cerio R, Gribben J, Lemoine N, Bomalaski J, Li CF, Joel S, Fitzgibbon J, Chen LT, Szlosarek PW: Promoter methylation of argininosuccinate synthetase-1 sensitises lymphomas to arginine deiminase treatment, autophagy and caspase-dependent apoptosis. Cell Death Dis 2012, 3: e342
5. Feun L, You M, Wu CJ, Kuo MT, Wangpaichitr M, Spector S, Savaraj N: Arginine deprivation as a targeted therapy for cancer. Curr Pharm Des 2008, 14:1049−1057
6. Feun L, Savaraj N: Pegylated arginine deiminase: a novel anticancer enzyme agent. Expert Opin Investig Drugs 2006, 15:815−822
7. Ascierto PA, Scala S, Castello G, Daponte A, Simeone E, Ottaiano A, Beneduce G, De Rosa V, Izzo F, Melucci MT, Ensor CM, Prestayko AW, Holtsberg FW, Bomalaski JS, Clark MA, Savaraj N, Feun LG, Logan TF: Pegylated arginine deiminase treatment of patients with metastatic melanoma: results from phase I and II studies. J Clin Oncol 2005, 23:7660−7668
8. Yang TS, Lu SN, Chao Y, Sheen IS, Lin CC, Wang TE, Chen SC, Wang JH, Liao LY, Thomson JA, Wang-Peng J, Chen PJ, Chen LT: A randomised phase II study of pegylated arginine deiminase (ADI-PEG 20) in Asian advanced hepatocellular carcinoma patients. Br J Cancer 2010, 103:954−960
9. Glazer ES, Piccirillo M, Albino V, Di Giacomo R, Palaia R, Mastro AA, Beneduce G, Castello G, De Rosa V, Petrillo A, Ascierto PA, Curley SA, Izzo F: Phase II study of pegylated arginine deiminase for nonresectable and metastatic hepatocellular carcinoma. J Clin Oncol 2010, 28:2220−2226
10. Szlosarek PW, Luong P, Phillips MM, Baccarini M, Stephen E, Szyszko T, Sheaff MT, Avril N: Metabolic response to pegylated arginine deiminase in mesothelioma with promoter methylation of argininosuccinate synthetase. J Clin Oncol 2013, 31:e111−e113
11. Bowles TL, Kim R, Galante J, Parsons CM, Virudachalam S, Kung HJ, Bold RJ: Pancreatic cancer cell lines deficient in argininosuccinate synthetase are sensitive to arginine deprivation by arginine deiminase. Int J Cancer 2008, 123:1950−1955
12. Kim RH, Coates JM, Bowles TL, McNerney GP, Sutcliffe J, Jung JU, Gandour-Edwards R, Chuang FY, Bold RJ, Kung HJ: Arginine deiminase as a novel therapy for prostate cancer induces autophagy and caspase-independent apoptosis. Cancer Res 2009, 69:700−708
13. Kelly MP, Jungbluth AA, Wu BW, Bomalaski J, Old LJ, Ritter G: Arginine deiminase PEG20 inhibits growth of small cell lung cancers lacking expression of argininosuccinate synthetase. Br J Cancer 2012, 106:324−332
14. Syed N, Langer J, Janczar K, Singh P, Lo Nigro C, Lattanzio L, Coley HM, Hatzimichael E, Bomalaski J, Szlosarek P, Awad M, O'Neil K, Roncaroli F, Crook T: Epigenetic status of argininosuccinate synthetase and argininosuccinate lyase modulates autophagy and cell death in glioblastoma. Cell Death Dis 2013, 4:e458
15. American Cancer Society: Cancer Facts & Figures 2014. Atlanta, American Cancer Society, 2014
16. Jemal A, Bray F, Center MM, Ferlay J, Ward E, Forman D: Global cancer statistics. CA Cancer J Clin 2011, 61:69−90
17. Gupta S, Hau AM, Beach JR, Harwalker J, Mantuano E, Gonias SL, Egelhoff TT, Hansel DE: Mammalian target of rapamycin complex 2 (mTORC2) is a critical determinant of bladder cancer invasion. PLoS One 2013, 8:e81081
18. Zhou N, Singh K, Mir MC, Parker Y, Lindner D, Dreicer R, Ecsedy JA, Zhang Z, Teh BT, Almasan A, Hansel DE: The investigational Aurora kinase A inhibitor MLN8237 induces defects in cell viability and cell-cycle progression in malignant bladder cancer cells in vitro and in vivo. Clin Cancer Res 2013, 19:1717−1728
19. Cline MS, Craft B, Swatloski T, Goldman M, Ma S, Haussler D, Zhu J: Exploring TCGA Pan-Cancer data at the UCSC Cancer Genomics Browser. Sci Rep 2013, 3:2652
20. Goldman M, Craft B, Swatloski T, Cline M, Morozova O, Diekhans M, Haussler D, Zhu J: The UCSC Cancer Genomics Browser: update 2015. Nucleic Acids Res 2015, 43:D812−D817
21. Vaske CJ, Benz SC, Sanborn JZ, Earl D, Szeto C, Zhu J, Haussler D, Stuart JM: Inference of patient-specific pathway activities from multi-dimensional cancer genomics data using PARADIGM. Bioinformatics 2010, 26:i237−i245
22. Cerami E, Gao J, Dogrusoz U, Gross BE, Sumer SO, Aksoy BA, Jacobsen A, Byrne CJ, Heuer ML, Larsson E, Antipin Y, Reva B, Goldberg AP, Sander C, Schultz N: The cBio cancer genomics portal: an open platform for exploring multidimensional cancer genomics data. Cancer Discov 2012, 2:401−404
23. Gao J, Aksoy BA, Dogrusoz U, Dresdner G, Gross B, Sumer SO, Sun Y, Jacobsen A, Sinha R, Larsson E, Cerami E, Sander C, Schultz N: Integrative analysis of complex cancer genomics and clinical profiles using the cBioPortal. Sci Signal 2013, 6:pl1
24. Cancer Genome Atlas Research Network: Comprehensive molecular characterization of urothelial bladder carcinoma. Nature 2014, 507: 315−322
25. Estes DA, Lovato DM, Khawaja HM, Winter SS, Larson RS: Genetic alterations determine chemotherapy resistance in childhood T-ALL: modelling in stage-specific cell lines and correlation with diagnostic patient samples. Br J Haematol 2007, 139:20−30
26. Palii SS, Kays CE, Deval C, Bruhat A, Fafournoux P, Kilberg MS: Specificity of amino acid regulated gene expression: analysis of genes subjected to either complete or single amino acid deprivation. Amino Acids 2009, 37:79−88
27. Ye J, Kumanova M, Hart LS, Sloane K, Zhang H, De Panis DN, Bobrovnikova-Marjon E, Diehl JA, Ron D, Koumenis C: The GCN2-ATF4 pathway is critical for tumour cell survival and proliferation in response to nutrient deprivation. EMBO J 2010, 29:2082−2096
28. Palam LR, Baird TD, Wek RC: Phosphorylation of eIF2 facilitates ribosomal bypass of an inhibitory upstream ORF to enhance CHOP translation. J Biol Chem 2011, 286:10939−10949
29. Allen MD, Luong P, Hudson C, Leyton J, Delage B, Ghazaly E, Cutts R, Yuan M, Syed N, Lo Nigro C, Lattanzio L, Chmielewska-Kassassir M, Tomlinson I, Roylance R, Whitaker HC, Warren AY, Neal D, Frezza C, Beltran L, Jones LJ, Chelala C, Wu BW, Bomalaski JS, Jackson RC, Lu YJ, Crook T, Lemoine NR, Mather S, Foster J, Sosabowski J, Avril N, Li CF, Szlosarek PW: Prognostic and therapeutic impact of argininosuccinate synthetase 1 control in bladder cancer as monitored longitudinally by PET imaging. Cancer Res 2014, 74:896−907
30. Kimura F, Florl AR, Seifert HH, Louhelainen J, Maas S, Knowles MA, Schulz WA: Destabilization of chromosome 9 in transitional cell carcinoma of the urinary bladder. Br J Cancer 2001, 85:1887−1893
31. Donnelly N, Gorman AM, Gupta S, Samali A: The eIF2alpha kinases: their structures and functions. Cell Mol Life Sci 2013, 70:3493−3511
32. Taylor SS, Haste NM, Ghosh G: PKR and eIF2alpha: integration of kinase dimerization, activation, and substrate docking. Cell 2005, 122: 823−825
33. Raven JF, Koromilas AE: PERK and PKR: old kinases learn new tricks. Cell Cycle 2008, 7:1146−1150
34. Chen JJ, London IM: Regulation of protein synthesis by heme-regulated eIF-2 alpha kinase. Trends Biochem Sci 1995, 20:105−108
35. Dever TE: Gene-specific regulation by general translation factors. Cell 2002, 108:545−556
36. Jewell JL, Russell RC, Guan KL: Amino acid signalling upstream of mTOR. Nat Rev Mol Cell Biol 2013, 14:133−139